Supporting information

Supramolecular chirality and symmetry breaking of fluoride complexes of achiral foldamers

Kaisa Helttunen, Riia Annala, Aku Suhonen, Elisa Nauha, Juha Linnanto, and Maija Nissinen

Table of Contents

1. Synthesis and characterization methods

All starting materials were commercially available and used as such unless otherwise noted. The glassware was dried at 120°C prior to use. Tetrahydrofurane (THF) was dried with MBraun solvent purification system. Triethylamine (Et_3N) was stored on molecular sieves (3 Å). NMR spectra were measured with a Bruker Avance DRX 500 spectrometer and the chemical shifts were calibrated to the residual proton and carbon resonance of the deuterated solvent. Melting points were measured in open capillaries using a Stuart Bibby Scientific SMP30 melting point apparatus and are uncorrected. High resolution ESI-TOF mass spectra were measured with a LCT Micromass spectrometer. Elemental analyses were done with a Vario EL III instrument.

Synthesis and crystal structures of aromatic oligoamides **1**, **2, 4** and **5** have been described in our previous papers.[1,2,3] The foldamer **3** with terminal *o*-nitrobenzoyl groups was synthesized in two steps by coupling 2-nitrobenzoic acid and *o*-phenylenediamine to produce *N*-(2-aminophenyl)-2-nitrobenzamide **7** (Scheme S-1). A subsequent reaction of **7** with pyridine-2,6-dicarbonyl dichloride produced foldamer **3** with a 29 % yield.

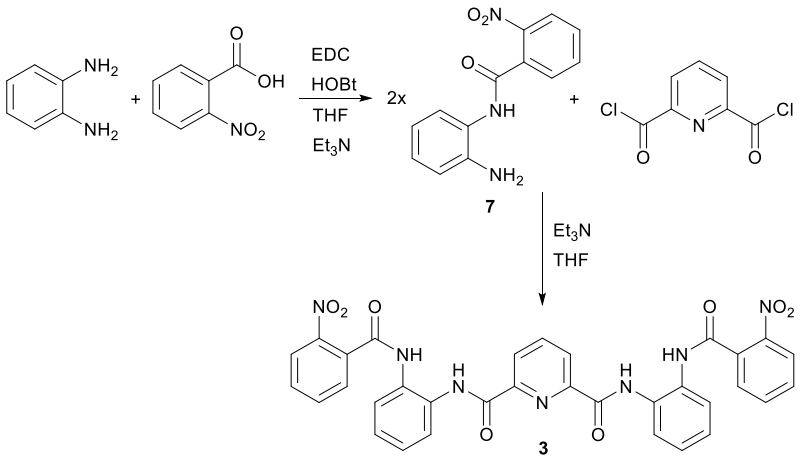

Scheme S-1. The reaction scheme for the synthesis of compounds **7** and **3**.

1.1. *N*-(2-aminophenyl)-2-nitrobenzamide 7

The synthesis was carried out under an argon atmosphere. *O*-phenylenediamine (633.4 mg; 5.86 mmol), 2-nitrobenzoic acid (326.0 mg; 1.95 mmol) and hydroxybenzotriazole hydrate (HOBt) (299.7 mg; 1.96 mmol) were dissolved in THF (100 ml). The solution was cooled to 0°C, and stirred for 30 minutes. Et_3N (0.30 ml; 2.15 mmol) and 1-ethyl-3-(3-

dimethylaminopropyl)carbodiimide (EDC) (0.40 ml; 2.26 mmol) were added to the solution. The cooled solution was stirred for 30 minutes, allowed to warm to RT and stirred overnight (20 h). The solution was concentrated as oil, dissolved in dichloromethane (DCM, 20 ml), and washed with deionized water (20 ml). The product **7** precipitated from DCM as a white powder and was filtered and washed with DCM and deionized water. Yield 219,7 mg (43.8 %). mp. 166-167 °C; ^{1}H NMR (500 MHz, DMSO-d_6, 30 °C): δ = 4.95 (s, 2H), 6.60 (td, $^{3}J_{HH}$ = 1.3 Hz, $^{3}J_{HH}$ = 7.5 Hz, 1H), 6.76 (dd, $^{3}J_{HH}$ = 1.3 Hz, $^{3}J_{HH}$ = 8.0 Hz, 1H), 6.98 (td, $^{3}J_{HH}$ = 1.4 Hz, $^{3}J_{HH}$ = 7.8 Hz, 1H), 7.24 (dd, $^{3}J_{HH}$ = 1.3 Hz, $^{3}J_{HH}$ = 8.0 Hz, 1H), 7.71-7.77 (m, 1H), 7.84-7.88 (m, 2H), 8.13 (d, $^{3}J_{HH}$ = 8.2 Hz, 1H), 9.93 (s, 1H), ^{13}C NMR (ESI†) (126 MHz, DMSO-d_6, 30 °C): δ = 115.80, 116.10, 122.16, 124.26, 126.15, 126.83, 129.56, 130.87, 132.82, 133.99, 142.88, 146.77, 164.49; HRMS (ESI+) *m/z*: $[M+Na]^+$ calcd for $[C_{13}H_{11}N_3O_3Na]$ 280.0693, found 280.0685, Δ = 2.9 ppm.

1.2. *N*^{2},*N*^{6}-bis(2-(2-nitrobenzamido)phenyl)pyridine-2,6-dicarboxamide 3

N-(2-aminophenyl)-2-nitrobenzamide **7** (170.1 mg; 0.66 mmol) was dissolved in THF (50 ml). The solution was stirred and Et_3N (0.10 ml; 0.72 mmol) was added to the solution. The solution was refluxed and pyridine-2,6-dicarbonyl dichloride (67.9 mg; 0.33 mmol) dissolved in THF (50 ml) was added slowly and dropwise to the mixture (1 h). The solution was refluxed for 30 min. A white precipitate formed in the solution (Et_3NHCl) was filtered. The filtrate was concentrated, dissolved in DCM (20 ml), washed with deionized water (3x20 ml) and brine (20 ml). The water and brine layers were combined and washed with DCM (35ml). The DCM phases were combined, dried with Na_2SO_4 and concentrated. The concentrated product was washed with EtOAc and filtered leaving the product **3** as a white powder. Yield 63.0 mg (29.5 %), mp. 262-263 °C; ^{1}H NMR (500 MHz, DMSO-d_6, 30 °C): δ = 7.23-7.30 (m, 4H), 7.52-7.62 (m, 8H), 7.66 (d, 2H, $^{3}J_{HH}$ = 7.4 Hz), 8.01 (dd, 2H, $^{3}J_{HH}$ = 0.8 Hz, $^{3}J_{HH}$ = 8.0 Hz), 8.30 (t, 1H, $^{3}J_{HH}$ = 7.7 Hz), 8.38 (d, 2H, $^{3}J_{HH}$ = 7.6 Hz), 10.49 (s, 2H), 10.86 (s, 2H) ppm; ^{13}C NMR (126 MHz, DMSO-d_6, 30 °C): δ 124.1, 124.9, 125.0, 125.3, 125.7, 125.8, 129.1, 130.2, 130.6, 130.8, 132.1, 133.8, 140.1, 146.1, 148.4, 161.3, 165.1; HRMS (ESI+) *m/z* $[M+Na]^+$ calcd for $[C_{33}H_{23}N_7O_8Na]$ 668.1500, found 668.1516, Δ=2.4 ppm.

2. Crystallography

Analytical grade solvents and *tetra*-butylammonium fluoride trihydrate (TBAF·$3H_2O$, 97 %) were used for crystallizations. Single crystal X-ray diffraction data were collected with an Agilent Supernova Dualsource diffractometer using an Agilent Atlas CCD detector and mirror monochromated CuK_α radiation (λ=1.5418 Å) except for the structure of **6_2-TBAF$_2$**, which was collected with Bruker Nonius KappaCCD diffractometer using Bruker AXS Apex II CCD detector and graphite monochromated CuK_α radiation (1.54178 Å). The structures were solved with direct methods and refined using Fourier techniques using SHELX-2014/6 or SHELX-2014/7 software package.[4] Analytical absorption correction was applied to all structures with CrysAlisPro[5] or with DENZO-SMN 1997[6] for **6_2-TBAF$_2$**. All non-hydrogen atoms were refined anisotropically except for some solvent carbon atoms in the structure **6_2-TBAF$_2$** (see Notes on the crystallographic data for details). All hydrogen atoms were refined isotropically and placed in idealized positions except for N-H hydrogen atoms which were found from the electron density map, and included in the structure factor calculations. Details of the crystal data, data collection and the refinement are presented in Tables S-1 and S-2. Graph set symbols[7,8] for hydrogen bonding were assigned and used to compare the hydrogen bonding between the different crystal structures when necessary.

Table S-1. Crystal data and collection parameters of foldamer **3** and the intermediate **7**

	3	**7**
Formula	$C_{33}H_{23}N_7O_8$	$C_{13}H_{11}N_3O_3$
Crystallization solvent	DMSO-d_6	EtOAc
M/gmol^{-1}	645.58	257.25
Crystal system	Monoclinic	Triclinic
Space group	$P2_1/c$	P-1
a/Å	14.96763(11)	7.4377(4)
b/Å	15.13591(11)	7.7862(4)
c/Å	12.96566(10)	11.4106(8)
α/°	90	75.345(6)
β/°	98.9550(7)	77.944(6)
γ/°	90	65.998(6)
V/Å^3	2901.55(4)	579.81(7)
Z	4	2
ρ_{calc}/g cm^{-3}	1.478	1.473
Meas. reflns	31292	10673
Indep. reflns	6089	4132
T/K	120	123
R_{int}	0.0336	0.0482
R_1 [I> 2σ(I)]	0.0341	0.0413
wR_2 [I> 2σ(I)]	0.0888	0.1119
GooF	1.044	1.020

Table S-2. Crystal data and collection parameters of the fluoride complexes.

	1-TBAF	**2-TBAF**	**3-TBAF**	**4-TBAF**	**5-TBAF**	**6_2-TBAF$_2$**
Formula	$C_{33}H_{25}N_5O_4 \cdot F \cdot C_{16}H_{36}N$	$2C_{34}H_{24}N_6O_4 \cdot 2F \cdot 2C_{16}H_{36}N \cdot 0.2H_2O$	$C_{33}H_{23}N_7O_8 \cdot F \cdot C_{16}H_{36}N$	$C_{26}H_{21}N_5O_3 \cdot F \cdot C_{16}H_{36}N$	$C_{26}H_{20}N_4O_3 \cdot F \cdot C_{16}H_{36}N$	$C_{26}H_{20}N_4O_3 \cdot F \cdot C_{16}H_{36}N \cdot C_3H_7NO$
Crystallization solvent	CH_3CN	$CDCl_3$	$CHCl_3$	Acetone-d_6	Acetone	DMF-CH_3CN
M/gmol^{-1}	817.03	1687.70	907.04	712.93	697.91	889.14
Crystal system	Orthorhombic	Monoclinic	Orthorhombic	Monoclinic	Monoclinic	Monoclinic
Space group	$P2_12_12_1$	$P2_1/n$	$Pca2_1$	$P2_1/c$	$P2_1/m$	$P2_1$
a/Å	11.16653(6)	16.80152(14)	19.61921(15)	19.7472(9)	8.94745(5)	13.9902(3)
b/Å	16.03601(10)	26.0097(3)	8.74681(5)	11.8235(6)	15.10359(11)	34.5843(10)
c/Å	24.54325(15)	22.2194(2)	27.9462(2)	16.8496(6)	14.92421(9)	21.6729(5)
α/°	90	90	90	90	90	90
β/°	90	108.6085(10)	90	92.177(4)	106.1554(6)	102.757(2)
γ/°	90	90	90	90	90	90
V/Å^3	4394.88(5)	9202.29(16)	4795.71(6)	3931.2(3)	1937.19(2)	10227.4(4)
Z	4	4	4	4	2	8
ρ_{calc}/g cm^{-3}	1.235	1.218	1.256	1.205	1.196	1.155
Meas. reflns	30278	52624	117930	15553	77272	28492
Indep. reflns	9228	18144	10087	8052	4229	15977
T/K	123	123	120	120	123	173
R_{int}	0.0210	0.0236	0.0440	0.0268	0.0344	0.1553
R_1 [I> 2σ(I)]	0.0320	0.0686	0.0418	0.0514	0.0378	0.1170
wR_2 [I> 2σ(I)]	0.0840	0.1747	0.1210	0.1332	0.1005	0.2890
GooF	1.020	1.096	1.060	1.024	1.004	1.038
Flack parameter	0.03(3)	-	0.28(5)	-	-	-0.1(4)

2.1. Notes on the crystallographic data

Foldamer **3** was crystallized from DMSO-d_6 by slow evaporation as colorless plate crystals. The missing five very strong reflections in fcf are caused by overflow.

Intermediate **7** was crystallized from EtOAc by recrystallization as colorless plate crystals. The crystal was twinned (two components, 44:56).

1-TBAF crystallized very slowly from acetonitrile at 1:5 molar ratio of **1** and TBAF as colorless irregular block crystals (Fig. S-1). The selected crystals were separated by cutting from a larger cluster. Data collection was performed for three different crystals, two of which with Mo radiation using Bruker Nonius Kappa CCD diffractometer and Bruker AXS Apex II CCD detector resulting in the same unit cell parameters as the reported structure. Stereochemistry was determined from the Flack parameters only for the reported crystal structure (measured with Cu radiation). The classic Flack was x = 0.035(122) and the Parsons' method Flack was x = 0.031(31). To confirm the reliable crystallization of the

complex and repeatability of supramolecular chirality the crystallization was repeated in the same conditions and with seed crystallization. The resulting crystals had the same space group and cell parameters as in the reported structure, which confirmed that fluoride complex forms reliably and repeatedly a chiral crystal structure.

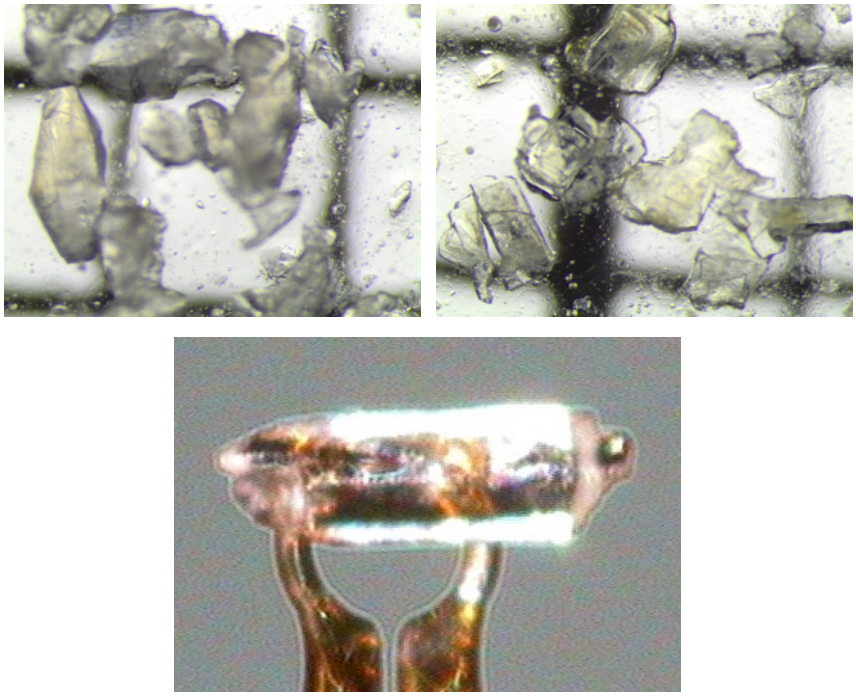

Figure S-1. Examples of microscope images of crystals: **1-TBAF** and **3-TBAF** at 32x magnification with 1 mm x 1 mm grid on the background (top) and **5-TBAF** crystal (size 0.390 × 0.123 × 0.071 mm^3; below).

2-TBAF was crystallized at 1:1 molar ratio of **2** and TBAF from $CDCl_3$ by slow evaporation as colorless block crystals. Short intermolecular contact between O101 and O500 indicates that electron density refined as an oxygen is indeed caused by a low occupancy water molecule in the structure. Occupancy of O500 was set as 20% to represent the low occupancy water molecule. The cyano group phenyl ring of molecule 1 is disordered over to positions (70:30) at O24-N26-C27-C28-C29-C30-C31-C32-C33-C34. One of the butyl chains of molecule 3 is disordered over two positions (87:13) at C01-C02. Short intramolecular hydrogen-hydrogen distance between H30F and H02Y is caused by the disorder of the butyl chain. Short intramolecular hydrogen-hydrogen distances between H21N and H205, and H11N and H105 are caused by an F…H11N or H21N ion-dipole bond. Bond lengths between C27A and O24A were restrained to 1.21 Å and between N102 and H12N to 0.87 Å using

DFIX. EADP and EXYZ restraints between C27A and C27B and an EADP restraint between O24A and O24B were used when modeling the molecule 1 disorder. Large Hirshfeld difference between C111 and C112 is caused by the molecule 1 disorder and a small void which are located nearby. The large non-solvent residue N U_{eq}(max)/U_{eq}(min) value is caused by the cyano group nitrogen atom N26 of the molecule 1 disorder. The (I_{obs}-I_{calc})/SigmaW > 10 outlier is likely caused by faults in the crystal. The structure contains voids of 14 Å^3.

3-TBAF was crystallized as colorless block crystals at 1:1 ratio of **3** and TBAF from $CHCl_3$ by slow evaporation (Fig. S-1). The large Hirshfeld difference between O8 and N7 is caused by slight disorder of the nitro group. Short intramolecular hydrogen-hydrogen distance between H3N and H4N is caused by ion-dipole bonds to the fluoride atom. The two (I_{obs}-I_{calc})/SigmaW > 10 outlier are likely caused by faults in the crystal. One of the butyl chains of the TBA-molecule is disordered over two positions (56:44) at C103-C104 (C13A-C14A, C13B-C14B). Bond lengths C13A-C14A and C13B-C14B were restrained to 1.54 Å and bond lengths N1-H1N and N2-H2N to 0.87 Å using DFIX. An EADP restraint between C14A and C14B was used when modeling the TBA-molecule disorder. The classic Flack x = 0.290(164) and the Parsons' method Flack x = 0.279(45). The relatively high su values mean that reliable conclusions can't be made.

4-TBAF was crystallized as yellow block crystals at 1:1 ratio of **4** and TBAF from acetone-d_6 by slow evaporation.

5-TBAF was crystallized at 1:1 ratio of **5** and TBAF from acetone by slow evaporation as colorless block crystals. The mirror symmetry is caused by the fact that the foldamer **5** is wrapped around the fluoride in a crescent shape in two different spatial positions in equal measure. The disorder could not be modeled with the whole foldamer mirrored in PART -1. Instead, only the end of the foldamer was constrained at 0.5 in PART -1. PART 1 and PART 2 were used for N5 and C1, with EADP and EXYZ restraints between them to model the disorder. Short intramolecular hydrogen-hydrogen distance between H1 and H2N is due to the disorder model. The large Hirshfeld difference between N5 and C2, N5 and C6, C1 and C2, C1 and C6 and between C2 and C11 is caused by the disorder in the main residue where the pyridine ring overlaps with an aromatic ring. Atoms constrained to 0.5 in PART 1 and PART

2 was used to model the disorder of the TBA residue. The large Hirshfeld difference between N7 and C34B is due to the disorder in the TBA residue.

6_2-TBAF_2 was crystallized at 1:1 ratio of **6** and TBAF from acetonitrile-DMF (1:1) mixture as colorless plates. Asymmetric unit contains two **6_2-TBAF_2** complexes and four DMF molecules. Low data completeness (86.0 %) is caused by poor crystal quality, which affects the quality of the structure. Thus, the structure can only be considered as preliminary. The refinement indicates partial solvent disorder, but no reasonable model could be built. C901-C903, C911-C913 and C935-C937 of solvents were refined isotropically. Void of 60 $Å^3$ with no electron density was observed between two TBA cations.

2.2. Hydrogen bonding parameters

Table S-3. Hydrogen bonding parameters for structures **3** and **7**.

3					
Intramolecular			**Intermolecular**		
Bond	**d(D···A)**	**<(DHA)**	**Bond**	**d(D···A)**	**<(DHA)**
N2-H2N···O4	3.3027	154.3(14)	N1-H1N···O2	2.9494(13)	171.7(15)
N2-H2N···N5	2.6560(13)	112.3(13)	N4-H4N···O3	2.8260(13)	175.7(16)
N3-H3N···O4	2.7512(13)	145.0(15)			
N3-H3N···N5	2.6950(14)	110.1(13)			
7					
Intramolecular			**Intermolecular**		
Bond	**d(D···A)**	**<(DHA)**	**Bond**	**d(D···A)**	**<(DHA)**
N3-H3NA···O3	3.103(2)	136.6(18)	N2-H2N···N3	2.9726(19)	161.1(19)
			N3-H3NB···O3	3.1889(17)	163.3(19)

Table S-4. Hydrogen bonding parameters for the foldamer fluoride complexes.

1-TBAF

Intramolecular			Intermolecular		
Bond	**d(D···A)**	**<(DHA)**	**Bond**	**d(D···A)**	**<(DHA)**
N4-H4···F1	2.7122(18)	156(3)	C46-H46A···O1	3.344(2)	156.3
N1-H1···F1	2.6815(18)	162(3)			
N5-H5···F1	2.6647(18)	160(3)			
N2-H2···F1	2.7403(18)	156(3)			

2-TBAF

Intramolecular			Intermolecular		
Bond	**d(D···A)**	**<(DHA)**	**Bond**	**d(D···A)**	**<(DHA)**
N101-H11N···F100	2.667(3)	163(3)			
N102-H12N···F100	2.742(3)	162(3)			
N103-H13N···F100	2.734(3)	152(3)			
N104-H14N···F100	2.617(3)	162(3)			
N102-H12N···N105	2.686(4)	106(2)			
N103-H13N···N105	2.681(4)	115(3)			
N201-H21N···F200	2.639(2)	158(2)			
N202-H22N···F200	2.693(2)	155(3)			
N203-H23N···F200	2.725(2)	157(3)			
N204-H24N···F200	2.619(2)	161(3)			
N202-H22N···N205	2.664(3)	111(2)			
N203-H23N···N205	2.654(3)	110(2)			

3-TBAF

Intramolecular			Intermolecular		
Bond	**d(D···A)**	**<(DHA)**	**Bond**	**d(D···A)**	**<(DHA)**
N1-H1N···F1	2.730(3)	154(4)			
N2-H2N···F1	2.629(3)	160(4)			
N3-H3N···F1	2.819(3)	163(4)			
N4-H4N···F1	2.592(3)	172(4)			
N2-H2N···N5	2.696(3)	110(3)			
N3-H3N···N5	2.670(3)	105(3)			

4-TBAF

Intramolecular			Intermolecular		
Bond	**d(D···A)**	**<(DHA)**	**Bond**	**d(D···A)**	**<(DHA)**
N1-H1N···F1	2.6092(17)	164(2)	N5-H5N2···O1	3.027(2)	168(3)
N2-H2N···F1	2.6313(17)	155(2)			
N3-H3N···F1	2.7908(19)	162(2)			
N5-H5N1···F1	2.7884(19)	165(3)			
N2-H2N···N4	2.664(2)	112(2)			
N3-H3N···N4	2.674(2)	108.5(19)			

5-TBAF

Intramolecular			Intermolecular		
Bond	**d(D···A)**	**<(DHA)**	**Bond**	**d(D···A)**	**<(DHA)**
N2-H2N···F1	2.6617(10)	163.9(11)			
N1-H1N···F1	2.8413(16)	162(2)			

Table S-4 **continued**

Intramolecular		
6_2-TBAF$_2$	**d(D···A)**	**<(DHA)**
N100-H10N···F1	2.724 (16)	158.8
N101-H11N···F1	2.692(15)	155.1
N200-H20N···F1	2.738(16)	148.9
N201-H21N···F1	2.746(14)	153.4
N102-H12N···F2	2.689(14)	152.9
N103-H13N···F2	2.679(16)	143.5
N202-H22N···F2	2.668(14)	154.3
N203-H23N···F2	2.724(15)	156.5
N300-H30N···F3	2.741(15)	156.3
N301-H31N···F3	2.702(14)	154.3
N400-H40N···F3	2.698(15)	152.1
N401-H41N···F3	2.713(14)	152.0
N302-H32N···F4	2.694(14)	155.3
N303-H33N···F4	2.675(14)	147.9
N402-H42N···F4	2.695(14)	150.5
N403-H43N···F4	2.744(15)	152.9

2.3. Intermolecular interactions and crystal packing

All intermolecular distances were measured with Mercury CSD 3.5.1.

The crystal structures of 3 and 7

Foldamer **3** folds in a relatively open conformation with only two intramolecular hydrogen bonds (S(7) and S(13)) and weak S(5) hydrogen bonds to the pyridine ring nitrogen (Figure S-2a). This leads to a complex packing structure where each foldamer forms four intermolecular hydrogen bonds to neighboring foldamers. Two of those bonds form a C(7) chain structure and the other two form a ring structure ($R_2^2(14)$, Figure S2b-c). These combine into a sheet structure as every other molecule of **3** in the C(7) chain connects to a chain on one side through the ring structure and every other molecule to a chain on the other side through the ring structure (Figure S-2c).

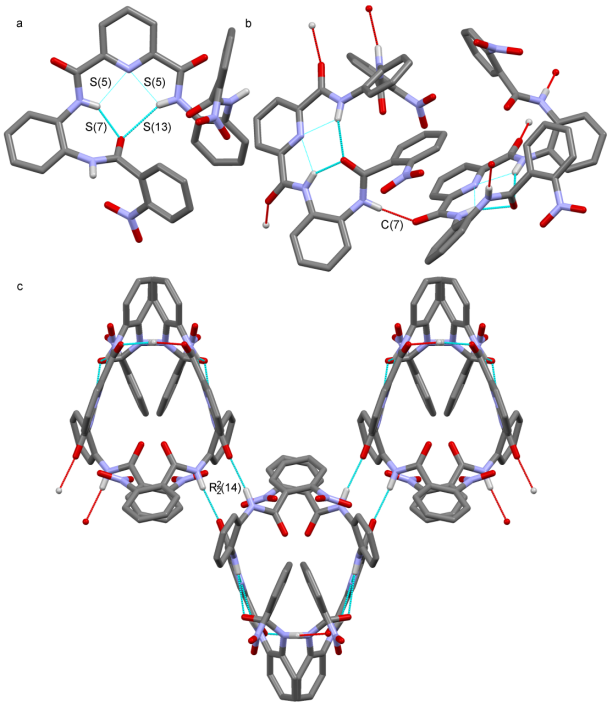

Figure S-2. The crystal structure of foldamer **3**. a) A single molecule in an open conformation, b) molecular chain packing (C(7)), c) molecular pair packing ($R_2^2(14)$) and the sheet structure with the molecular chains perpedicular to the viewing plane. Non-contact hydrogen atoms removed for clarity.

Compound **7** is an intermediate product in the synthesis of foldamer **3**. The compound has one intramolecular hydrogen bond (S(7), Figure S-3a) and a packing structure composed of two ring structures ($R_2^2(10)$ and $R_2^2(14)$) that form a molecular chain structure ($C_4^4(18)$, Figure S-3b).

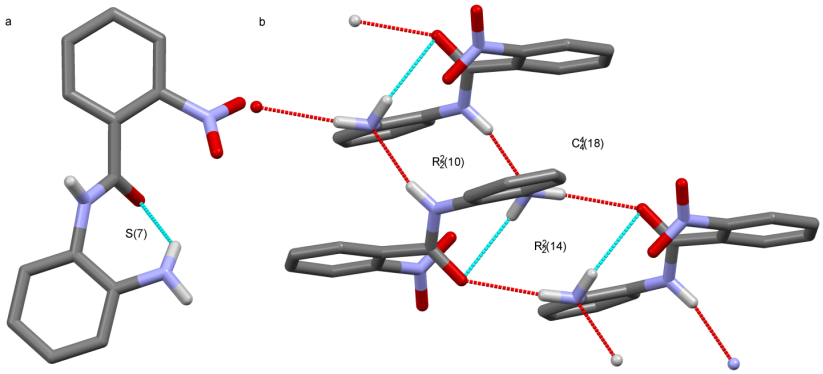

Figure S-3. The crystal structure of the reaction intermediate **7**: a) single molecule, b) crystal packing. Non-contact hydrogen atoms removed for clarity.

The crystal structures of the fluoride complexes

2-TBAF

In the structure of **2-TBAF** the molecular pairs are formed via aromatic interactions (edge-to-face and offset face-to-face; Figure S-4). The pairs are surrounded by TBA cations and a molecule of water.

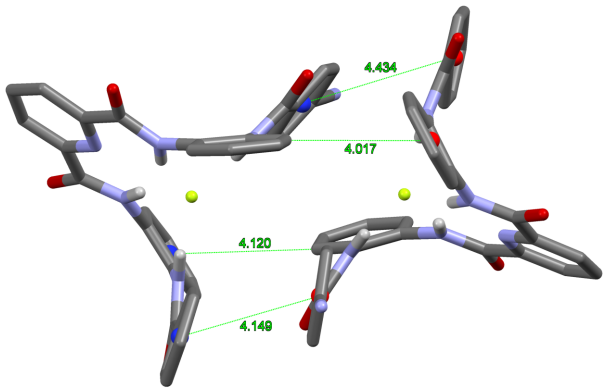

Figure S-4. 2-TBAF molecular pair connected by aromatic interactions (selected interactions shown). Disorder of the cyano group containing phenyl ring of the foldamer on the left, cations, water and non-contact hydrogen atoms were removed for clarity.

3-TBAF

Foldamer **3**-fluoride complexes are connected to a chain by weak ion-dipole interactions between pyridine ring hydrogen and a fluoride ion (Fig. S-4). The chains only contain either left- or right-handed complexes and are parallel with b-axis of the unit cell.

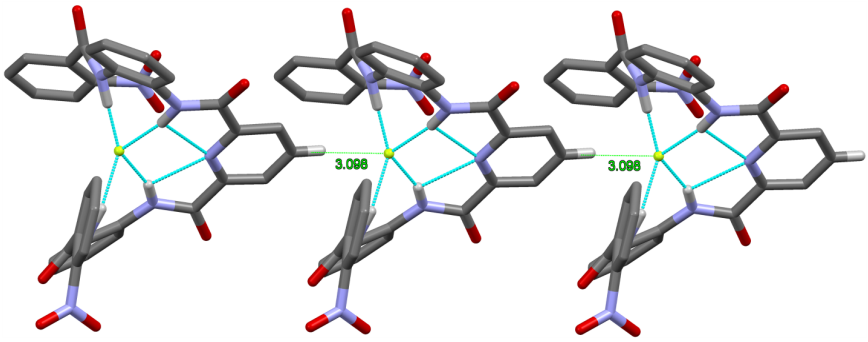

Figure S-5. Crystal packing of foldamer **3** in the structure **3-TBAF**. Non-contact hydrogen atoms were removed for clarity.

4-TBAF

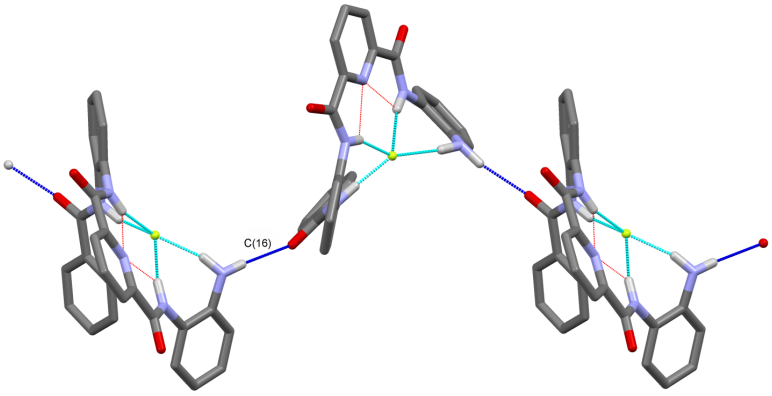

Figure S-6. Crystal packing in the structure **4-TBAF** is based on hydrogen bonded chains. Non-contact hydrogen atoms were removed for clarity.

6_2-TBAF$_2$

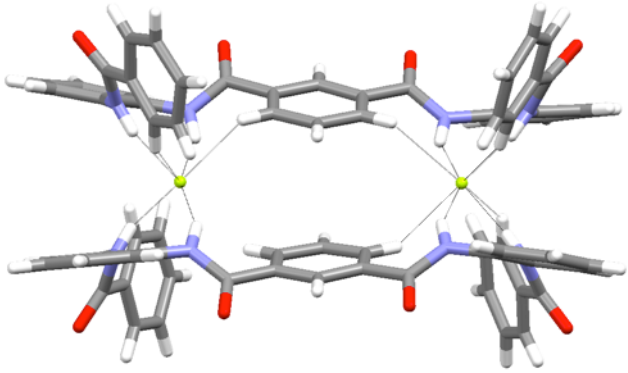

Figure S-7. The structure of foldamer **6_2-TBAF$_2$** dimeric complex. TBA cations and solvent DMF are excluded for clarity.

3 UV-vis and CD-spectroscopy

Solution sample of foldamer **1** and TBAF was prepared in THF, and a crystal of **1-TBAF** was dissolved in THF. For the solid state measurements altogether 10 crystals were screened by determining their unit cells with single crystal X-ray diffraction. Two of these were of poor quality and eight were the expected crystal form based on their unit cells. Four of these crystals were large enough for the measurements and three of them were used for solid state measurements and one for the solution measurement (see above). The samples of **1-TBAF** were prepared in KCl tablets as follows: bulk sample 0.512 mg/99.822 mg KCl, crystal 1 0.090 mg/99.332 mg KCl, crystal 2 0.232 mg/100.188 mg KCl, and crystal 3 0.068 mg/98.912 mg KCl.

Solution state UV-vis spectra were measured with Perkin Elmer Lambda 850 spectrophotometer in a quartz cuvette and solid state UV-vis spectra with JASCO V-670 spectrophotometer in a KCl tablet (Fig. S-8).

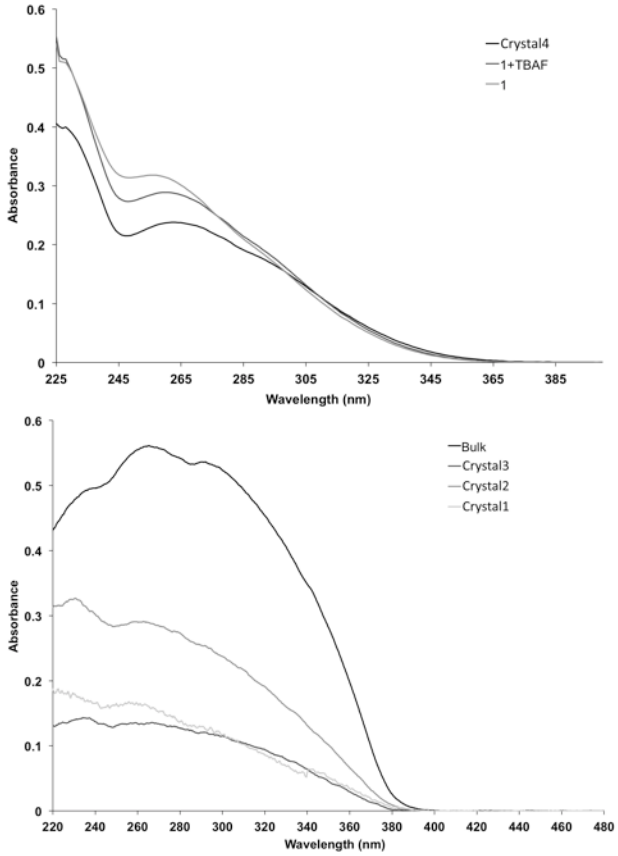

Figure S-8. Top: UV-vis spectra dissolved crystal of **1-TBAF** (3 ml of THF), 1:1 mixture of **1** and TBAF solutions in THF (10 μM for **1**), and 10 μM solution of **1**. Bottom: Solid state UV-vis spectra of **1-TBAF** bulk sample and single crystals.

CD spectra were measured with JASCO J-715 spectropolarimeter in a 10 mm quartz cuvette in THF (Figure S-9) and solid state CD spectra with JASCO J-810 spectropolarimeter in a KCl tablet. Figures of the single crystals of **1-TBAF** used in the measurements are shown in Fig. S-10.

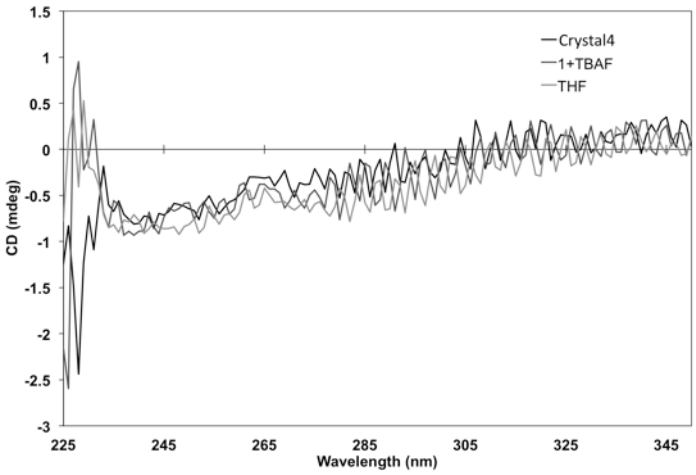

Figure S-9. CD spectra of dissolved crystal of **1**-TBAF in THF, 1:1 mixture of **1** and TBAF solutions in THF (10 μM for **1**), and THF.

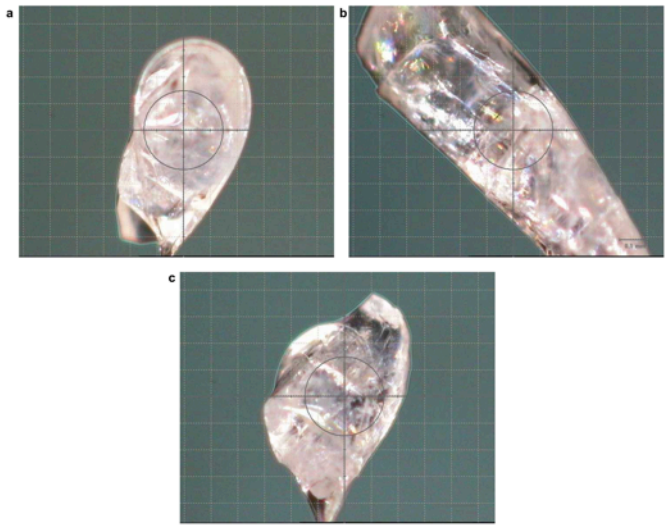

Figure S-11. Microscope pictures of crystal 1 (a, size 0.70 × 0.45 × 0.40 mm^3), crystal 2 (b, size >1.00 × 0.50 × 0.50 mm^3) and crystal 3 (c, size 0.75 × 0.40 × 0.30 mm^3) of **1-TBAF** used in the solid state measurements.

4 Calculated CD spectra

3*2*1 supercell structure from the X-ray structure of **1-TBAF** was used as a structural model to calculate CD spectra of solid state 1-TBAF. Both time-dependent (TD) density functional CAM-B3LYP and semiempirical configuration interaction ZINDO/S CIS methods were used in the spectral calculations. TD-CAM-B3LYP/6-311G(d,p) method using Gaussian 09 program[9] was used to calculate low energy transitions (below 43500 cm^{-1} (230 nm)) whereas ZINDO/S CIS method using ArgusLab program[10] was used to calculate higher transitions. To generate CD spectral shape, Gaussian line shape function of widths (full width at half maximum) of 3000 and 5000 cm^{-1} were used for calculated transitions in spectral regions of 100-225 and 225-500 nm, respectively.

5 NMR spectra

^{1}H NMR spectrum of 7

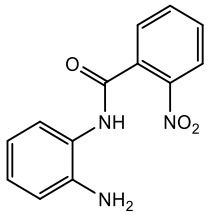

7

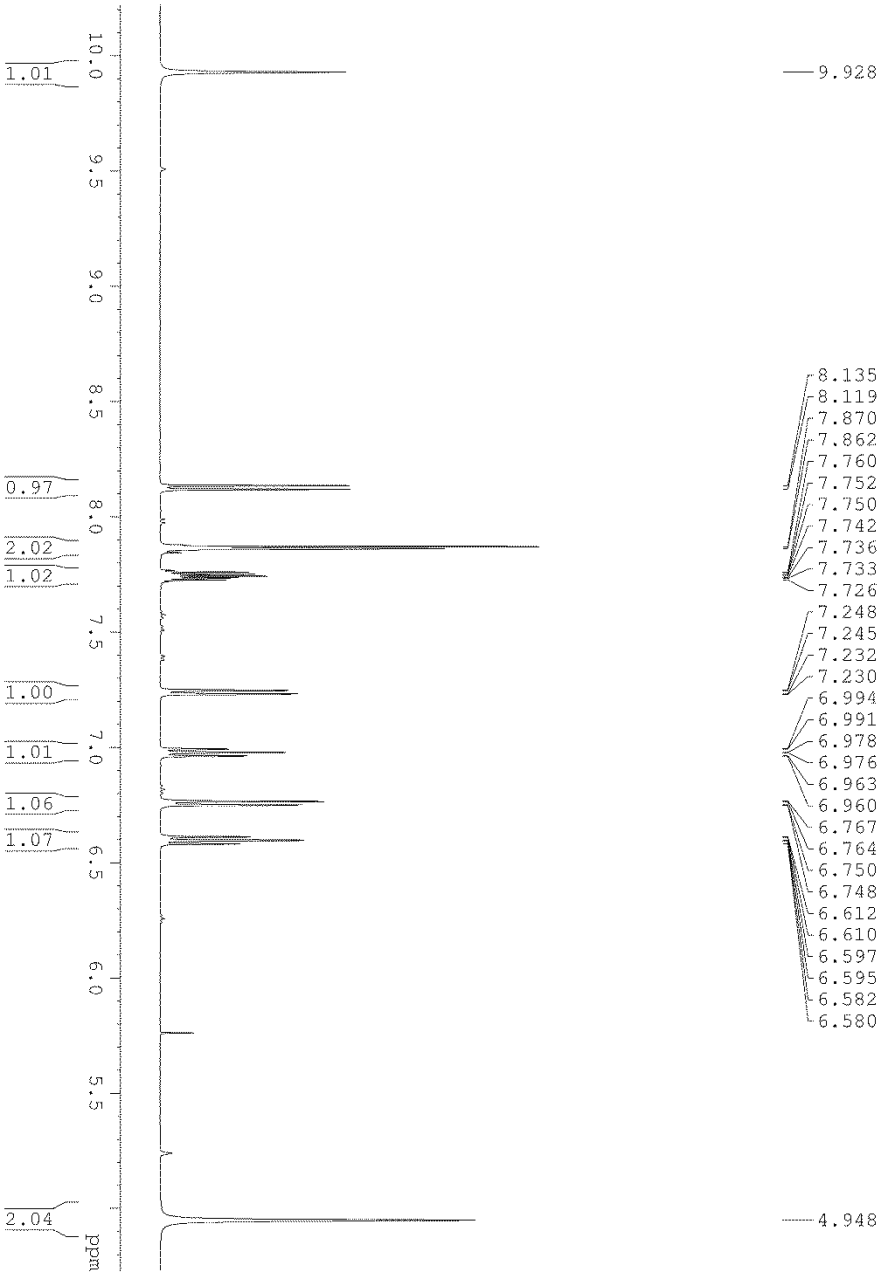

^{1}H NMR spectrum of 7: an expansion of the aromatic region

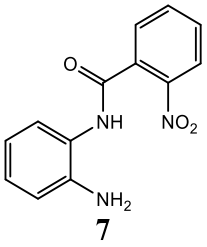

7

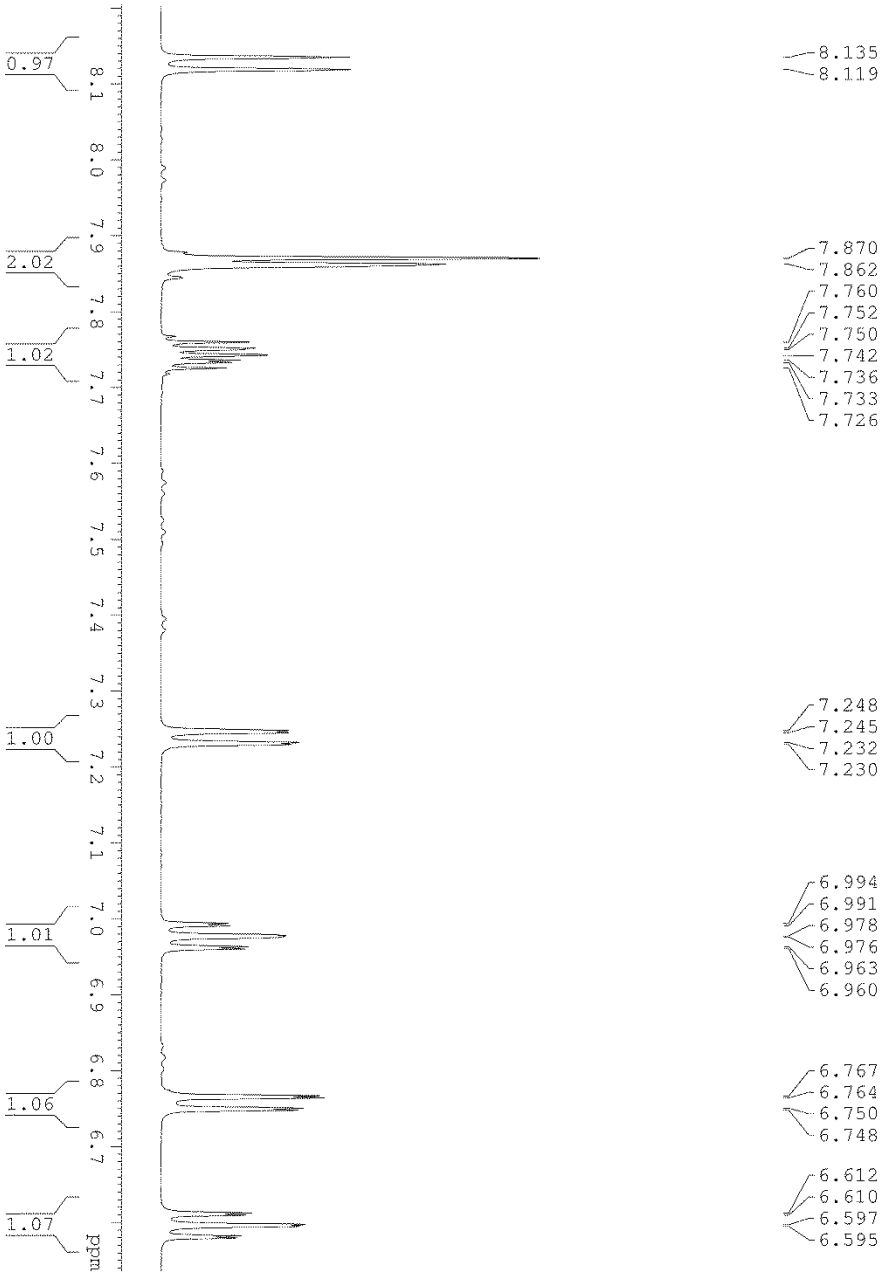

^{13}C NMR spectrum of 7

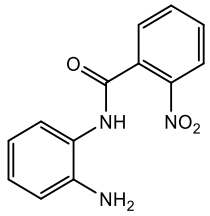

7

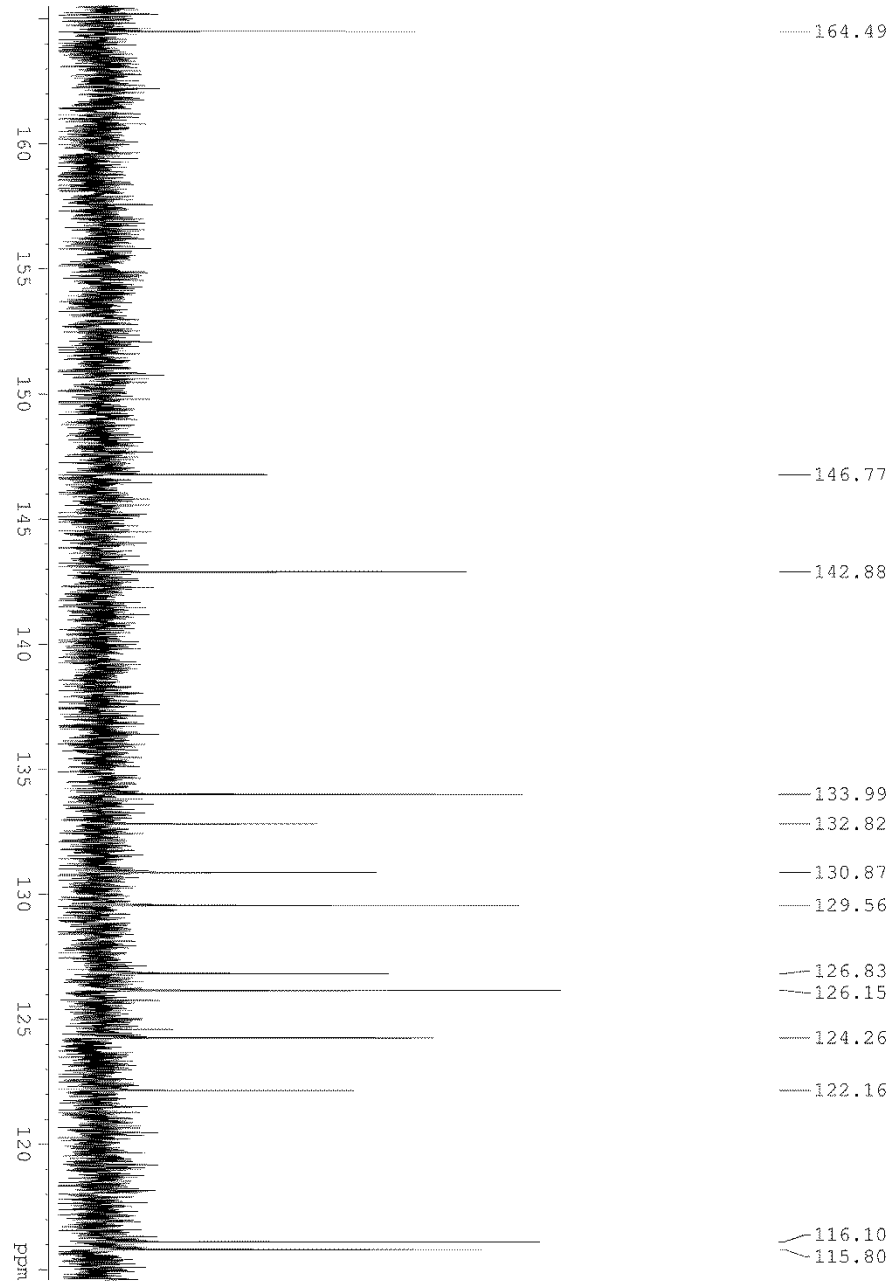

^{1}H NMR spectrum of 3

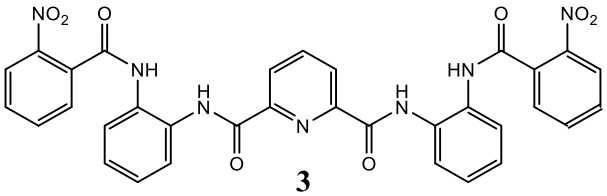

3

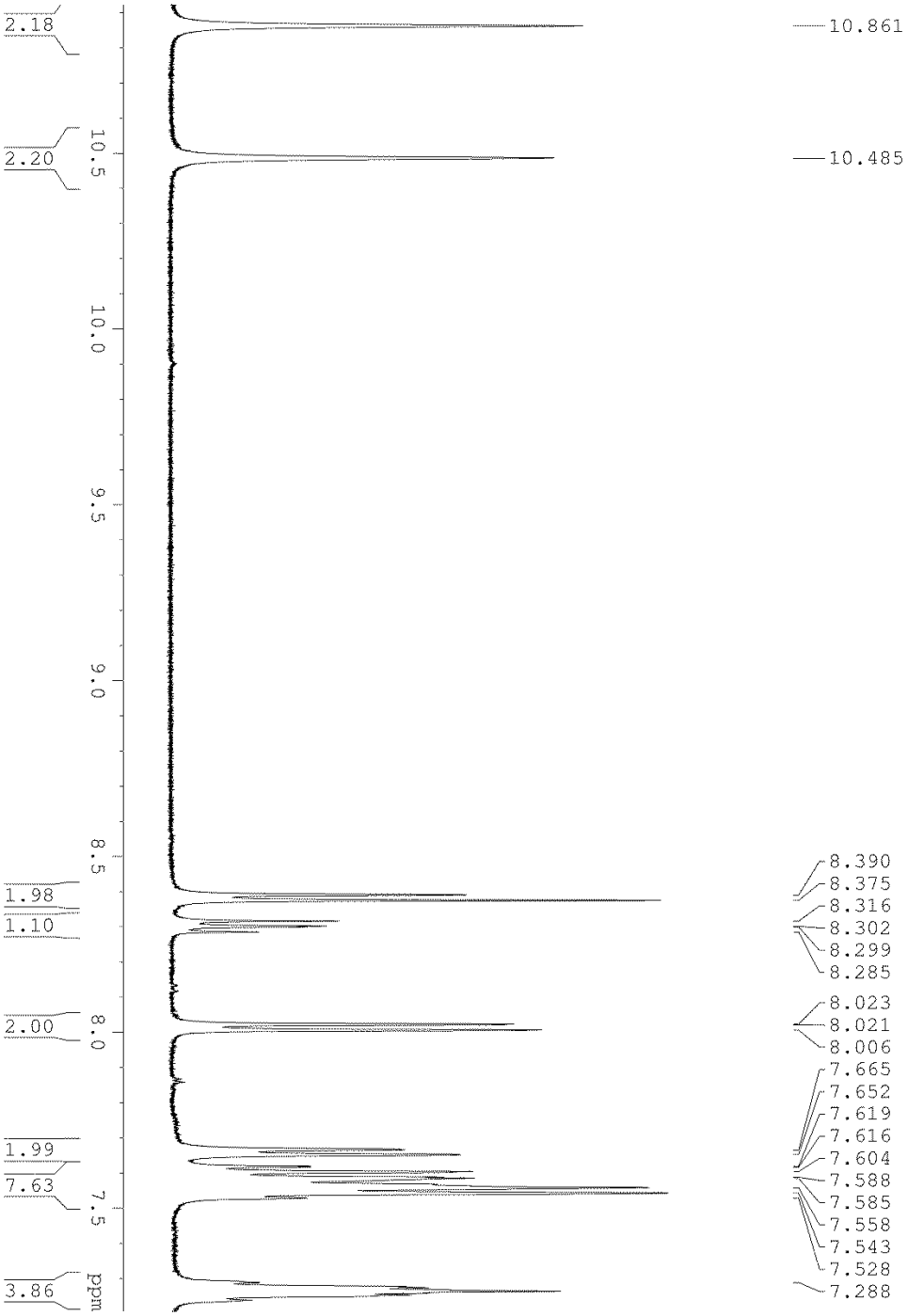

^{1}H NMR spectrum of 3: an expansion of the aromatic region

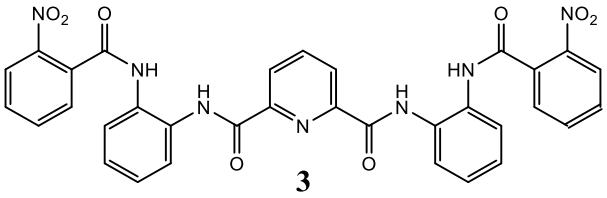

3

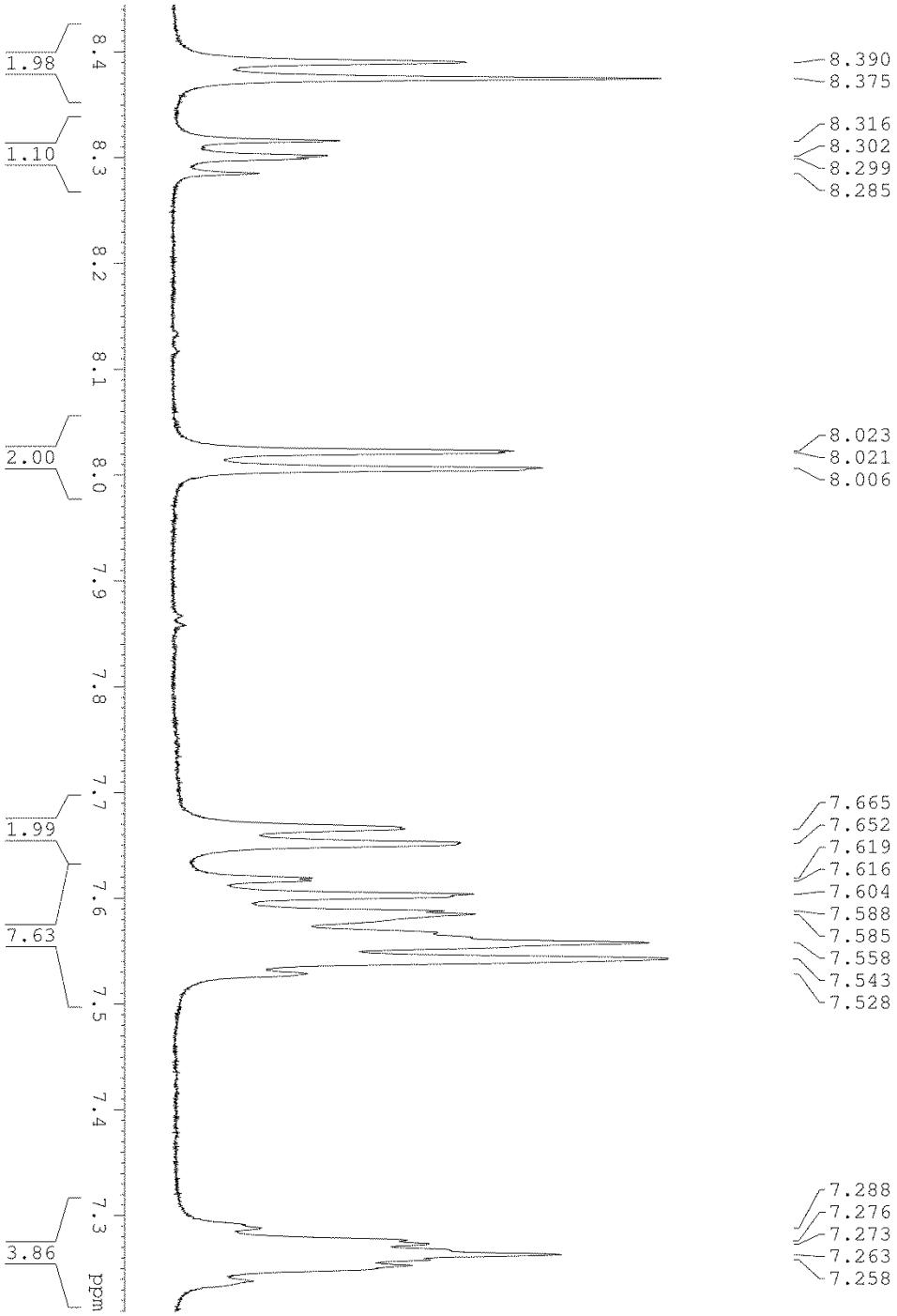

^{13}C NMR spectrum of 3

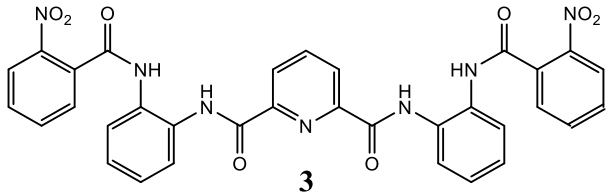

3

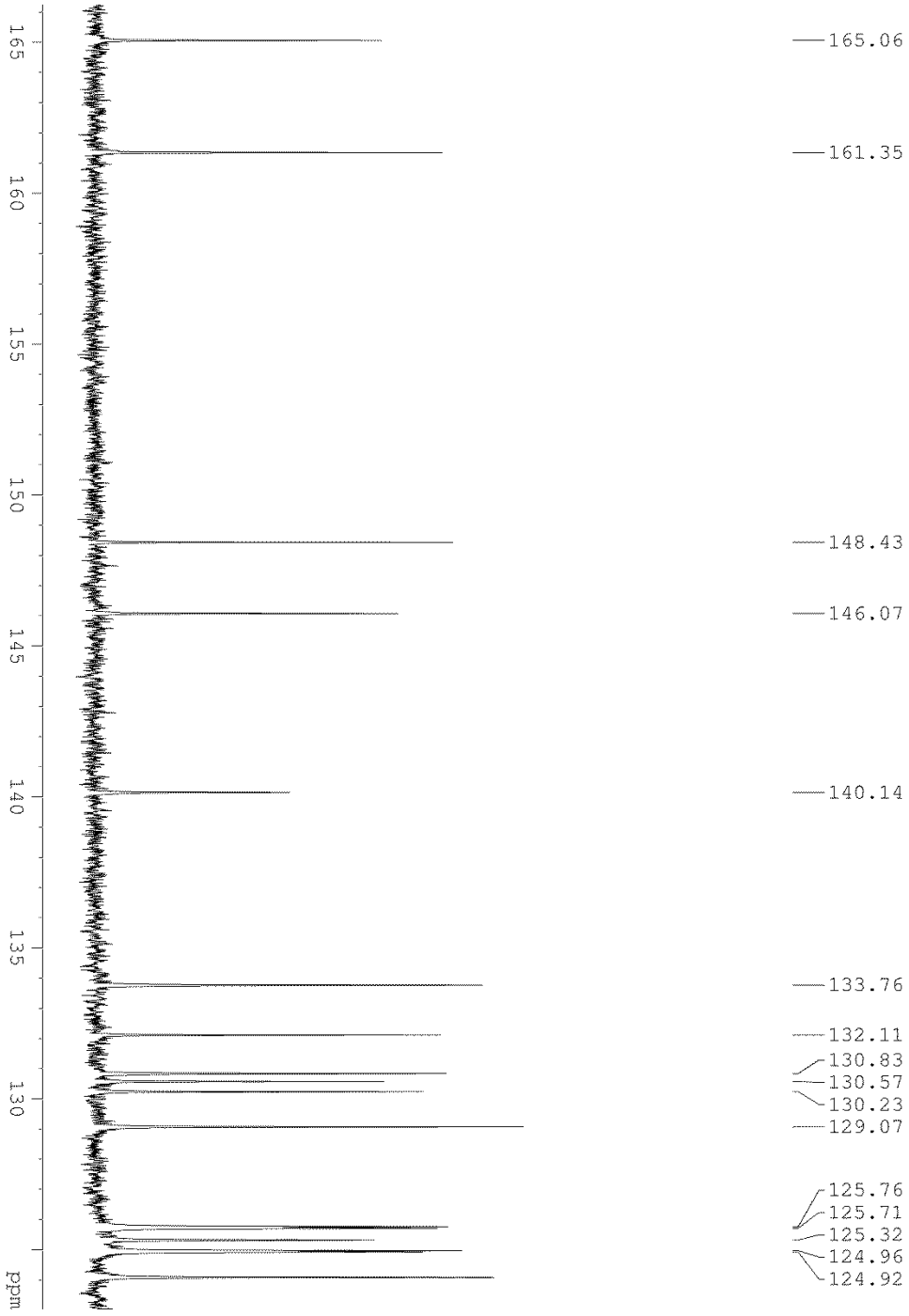

^{13}C NMR spectrum of 3: an expansion

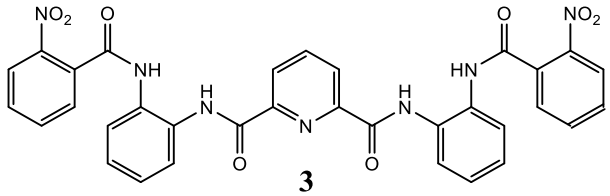

3

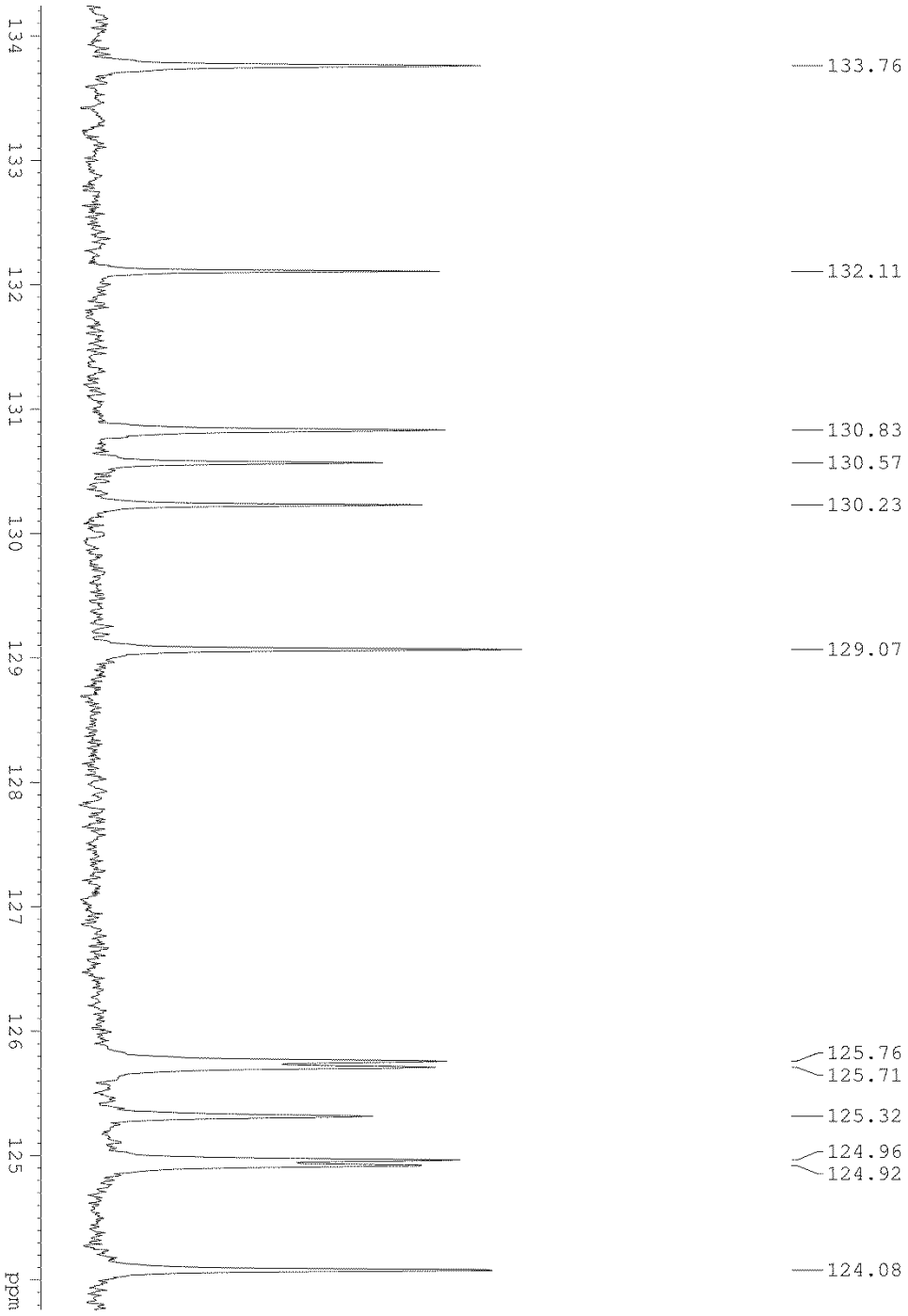

COSY spectrum of 3

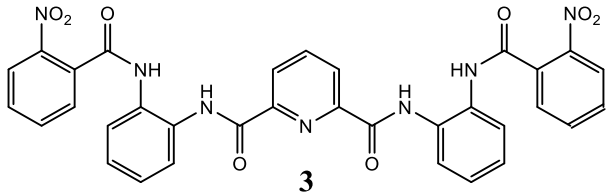

3

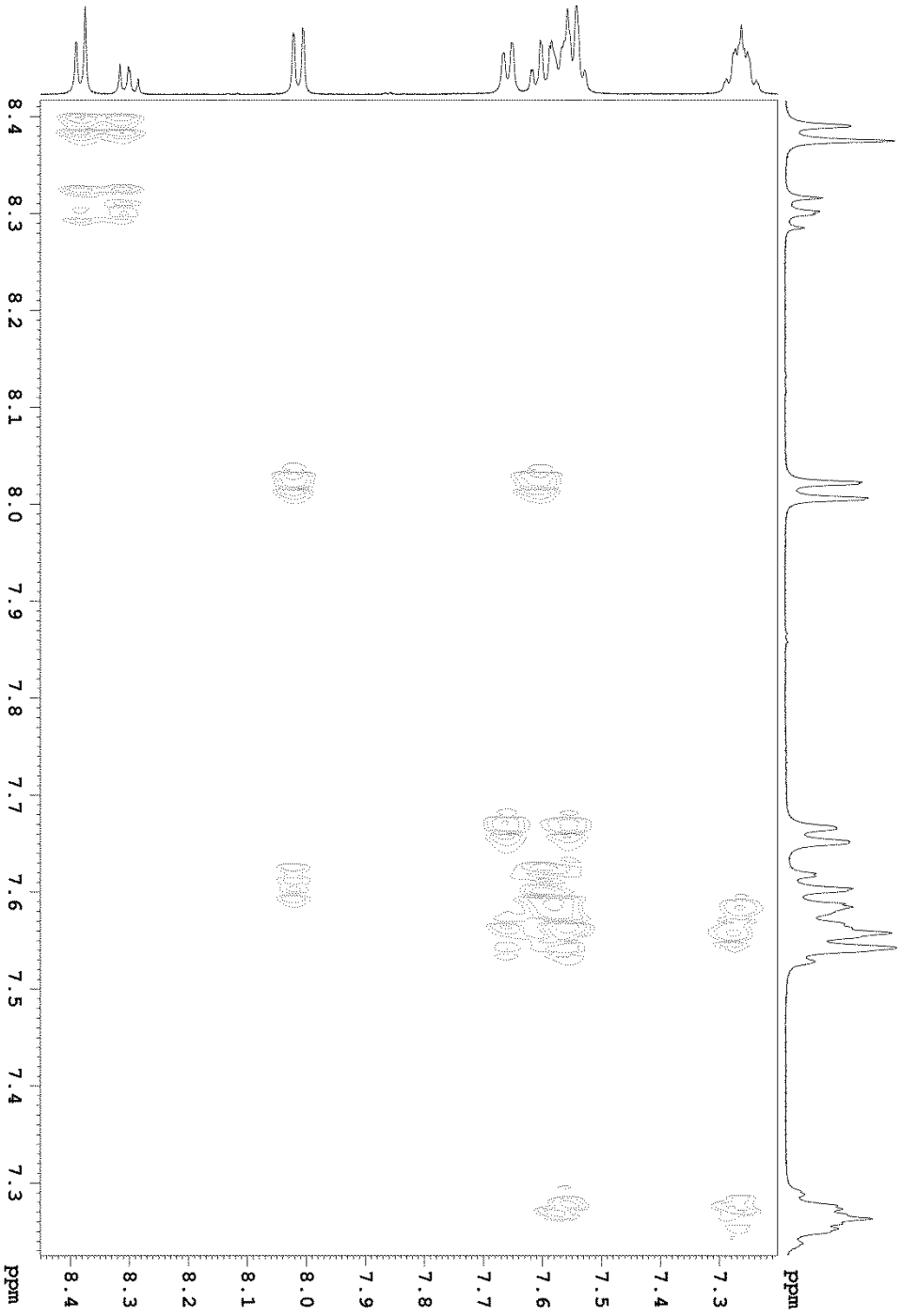

HMQC spectrum of 3

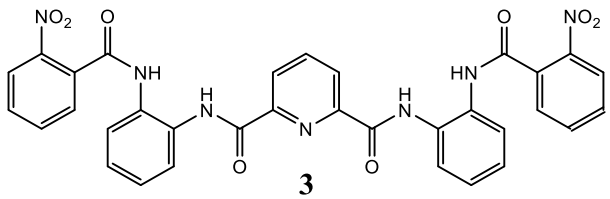

3

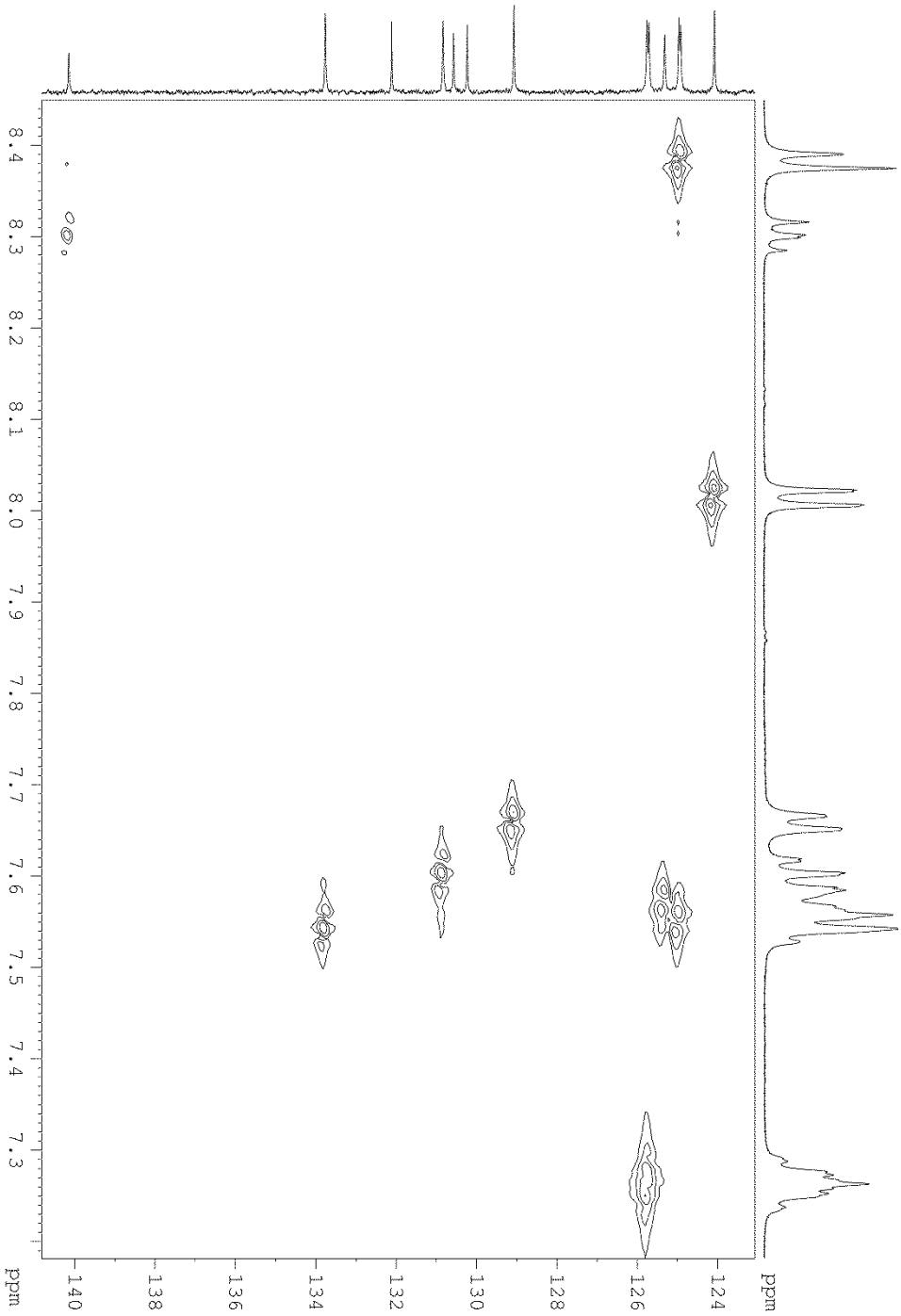

HMBC spectrum of 3

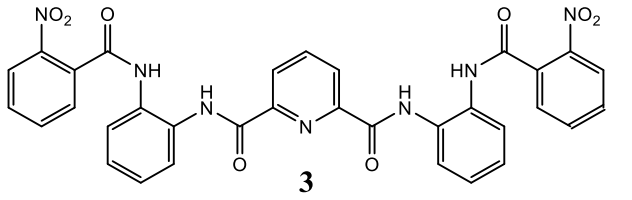

3

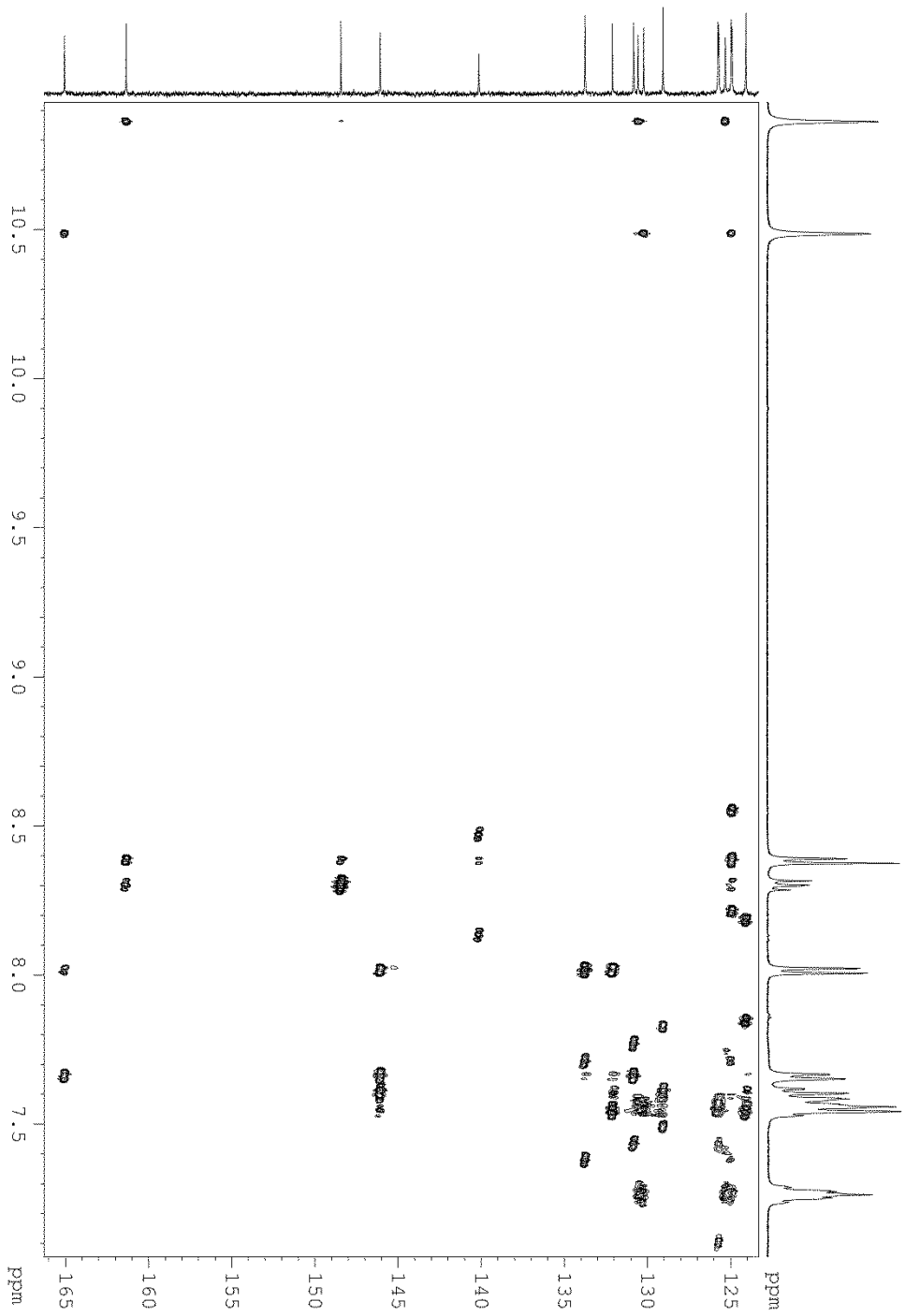

HMBC spectrum of 3: expansion

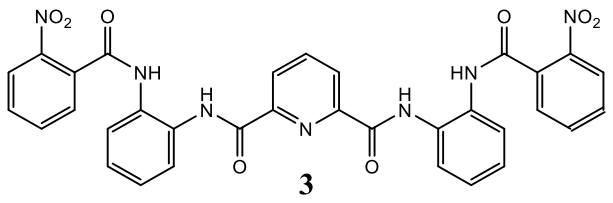

3

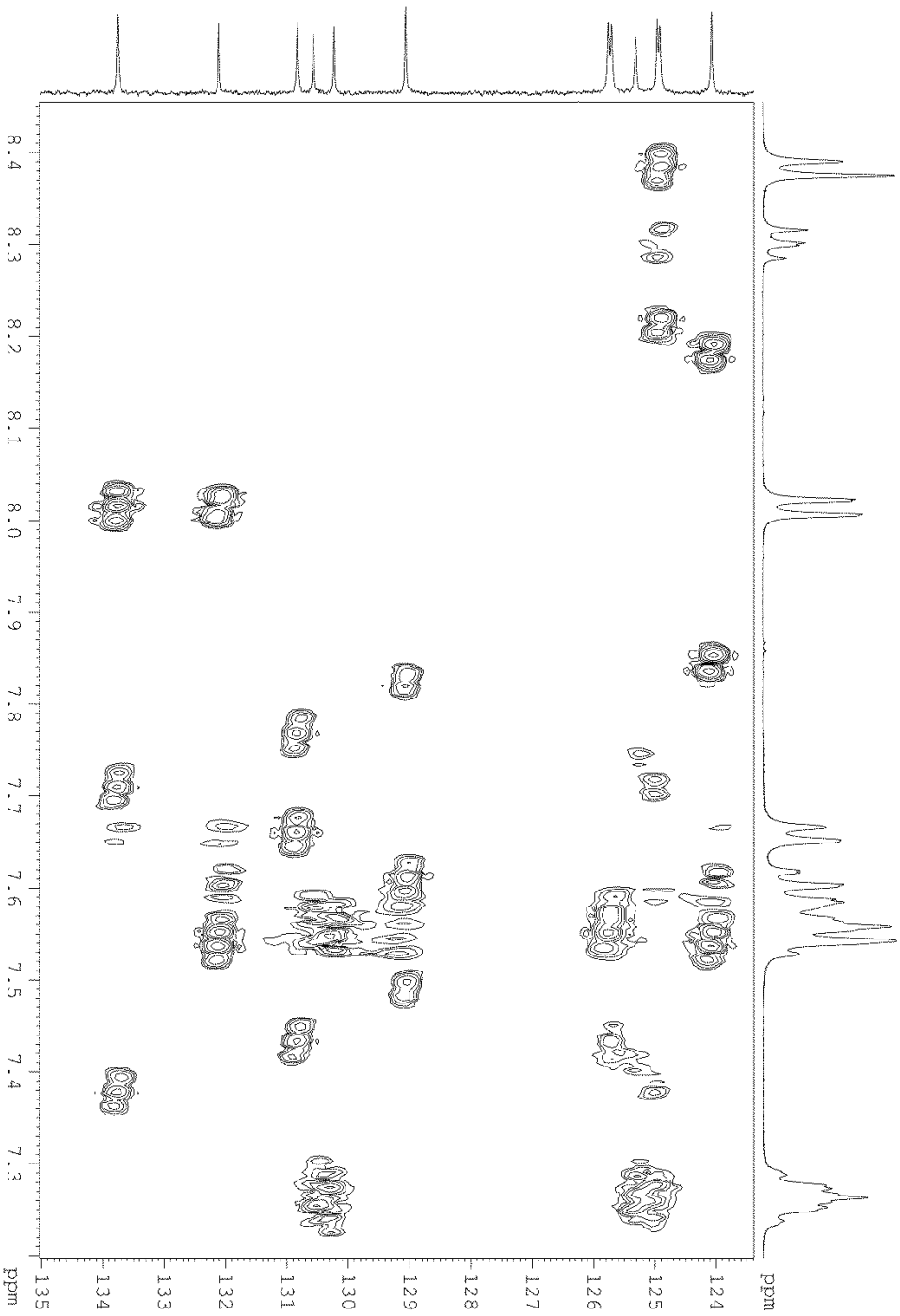

References

[1] A. Suhonen, E. Nauha, K. Salorinne, K. Helttunen, and M. Nissinen, *CrystEngComm*, 2012, **14**, 7398–7407.

[2] M. Kortelainen, A. Suhonen, A. Hamza, I. Pápai, E. Nauha, S. Yliniemelä-Sipari, M. Nissinen, and P. M. Pihko, *Chem. - A Eur. J.*, 2015, **21**, 9493–9504.

[3] A. Suhonen, M. Kortelainen, E. Nauha, S. Yliniemelä-Sipari, P. M. Pihko, and M. Nissinen, *CrystEngComm*, 2016, **18**, 2005–2013.

[4] G. M. Sheldrick, *Acta Crystallogr. A.*, 2008, **64**, 112.

[5] Agilent (2011), CrysAlisPRO, Agilent Technologies UK Ltd, Yarnton, England.

[6] Z. Otwinowski, D. Borek, W. Majewski and W. Minor, *Acta Crystallogr. A.*, 2003, **59**, 228.

[7] M. C. Etter and J. C. MacDonald, *Acta Crystallogr., Sect. B: Struct. Sci.*, 1990, **46**, 256.

[8] J. Bernstein, R. E. Davis, L. Shimoni and N.-L. Chung, *Angew. Chem., Int. Ed.*, 1995, **34**, 1555.

[9] M. J. Frisch, G. W. Trucks, H. B. Schlegel, G. E. Scuseria, M. A. Robb, J. R. Cheeseman, G. Scalmani, V. Barone, B. Mennucci, G. A. Petersson, H. Nakatsuji, M. Caricato, X. Li, H. P. Hratchian, A. F. Izmaylov, J. Bloino, G. Zheng, J. L. Sonnenberg, M. Hada, M. Ehara, K. Toyota, R. Fukuda, J. Hasegawa, M. Ishida, T. Nakajima, Y. Honda, O. Kitao, H. Nakai, T. Vreven, J. A. Montgomery, Jr., J. E. Peralta, F. Ogliaro, M. Bearpark, J. J. Heyd, E. Brothers, K. N. Kudin, V. N. Staroverov, T. Keith, R. Kobayashi, J. Normand, K. Raghavachari, A. Rendell, J. C. Burant, S. S. Iyengar, J. Tomasi, M. Cossi, N. Rega, J. M. Millam, M. Klene, J. E. Knox, J. B. Cross, V. Bakken, C. Adamo, J. Jaramillo, R. Gomperts, R. E. Stratmann, O. Yazyev, A. J. Austin, R. Cammi, C. Pomelli, J. W. Ochterski, R. L. Martin, K. Morokuma, V. G. Zakrzewski, G. A. Voth, P. Salvador, J. J. Dannenberg, S. Dapprich, A. D. Daniels, O. Farkas, J. B. Foresman, J. V. Ortiz, J. Cioslowski, and D. J. Fox, *Gaussian 09, Revision D.01, Gaussian, Inc., Wallingford CT*, 2013.

[10] Mark A. Thompson*, ArgusLab 4.0*, Planaria Software LLC, Seattle, WA.